This is a preprint, the final version is subject to change, of the American Mineralogist (MSA)
Cite as Authors (Year) Title. American Mineralogist, in press.
(DOI will not work until issue is live.) DOI: http://dx.doi.org/10.2138/am.2013.4259

Revised version #4259R

Superstructure, crystal chemistry and cation distribution in filipstadite, a Sb^{5+} - bearing, spinel-related mineral

PAOLA BONAZZI*, LAURA CHELAZZI, LUCA BINDI

Dipartimento di Scienze della Terra, Università di Firenze, Via La Pira 4, I-50121 Firenze, Italy

ABSTRACT

The crystal structure of the rare, spinel-related Sb mineral filipstadite from Långban, Filipstad district, Värmland, Sweden, has been solved and refined in the space group $Fd\bar{3}m$ [a = 25.9300(6) Å, V = 17434.4(5) Å^3, Z = 216] and refined to R = 4.41% for 681 $F_o > 4\sigma(F_o)$ using Mo$K\alpha$ X-ray data. The structure of filipstadite is topologically identical to the spinel-type structure with cations occupying 1/8 of the tetrahedral (T) and 1/2 of the octahedral (M) interstices of a cubic close-packing of oxygen atoms. Due to the cation ordering, which leads to the tripling of the unit-cell edge, the M and T sites of the spinel-type structure split into six and five independent sites, respectively. Chemical composition was determined by electron microprobe. The fractions of major cations obtained from chemical analysis were distributed between T and M sites taking into account the weighted electron number at both T and M sites, and minimizing the discrepancy between the calculated and the observed overall <M-O> distance. Cations present in minor amounts were assigned on the basis of their known site preference. The obtained populations (2M = $Mn^{2+}_{0.56}Mg_{0.76}Fe^{3+}_{0.16}Al_{0.02}Sb^{5+}_{0.50}$; T = $Mn^{2+}_{0.60}Mg_{0.07}Fe^{3+}_{0.30}Zn_{0.02}Si^{4+}_{0.01}$) were then tentatively distributed among the individual M and T sites on the basis of crystal chemical considerations.

Key words: filipstadite; spinel; crystal structure determination; superstructure; cation distribution; Långban (Sweden).

INTRODUCTION

Filipstadite, ideally $(Mn^{2+},Mg)_2(Fe^{3+}_{0.5}Sb^{5+}_{0.5})O_4$, was first described by Dunn et al. (1988) as a new spinel-related mineral having orthorhombic symmetry and unit cell parameters $a = 36.7$, $b = 36.7$, $c = 25.9$ Å. Using Weissenberg and precession methods, Dunn et al. showed a substructure-superstructure relationship with intense reflections corresponding to those of spinel-type structure ($a = 3\sqrt{2}a_s$, $b = 3\sqrt{2}a_s$ and $c = 3a_s$, where a_s is the unit-cell translation of a spinel-type structure) and supposed the superstructure to be due to cation ordering at the octahedral sites. This reasonable hypothesis, however, remained to be proved by a structure analysis.

At the type-locality (Långban, Filipstad district, Värmland, Sweden) filipstadite occurs intimately associated with jacobsite, ingersonite and calcite. In particular, filipstadite was described to replace jacobsite, $(Mn^{2+},Fe^{2+},Mg)(Fe^{3+},Mn^{3+})_2O_4$, and many filipstadite crystals were reported as having residual, irregular cores of jacobsite. Two other occurrences of filipstadite were later reported at two other 'Långban-type' Mn-Fe deposits, namely Jakobsberg and Nordmark, in south-central Sweden (Holtstam 1993; Holtstam et al. 1998). At Jakobsberg the mineral coexists with hausmannite, calcite, forsterite, phlogopite and another spinel-related phase exhibiting close similarities with filipstadite (Holtstam 1993) which was later approved as a new mineral species with the name tegengrenite (Holtstam and Larsson 2000). At Nordmark filipstadite occurs in fine-grained rock samples, including arsenates of svabite-johnbaumite and adelite-tilasite series, forsterite, phlogopite, manganoan calcite, plumbiam stibarsen and plumbian romeite (Holtstam et al. 1998). Interestingly, in the Nordmark samples described by Holtstam et al. (1998), Sb-poor filipstadite and Sb-rich jacobsite occur, possibly indicating solid solution between jacobsite-magnesioferrite spinel

This is a preprint, the final version is subject to change, of the American Mineralogist (MSA)
Cite as Authors (Year) Title. American Mineralogist, in press.
(DOI will not work until issue is live.) DOI: http://dx.doi.org/10.2138/am.2013.4259

and filipstadite. As pointed out by these authors, however, the crystallographic features of filipstadite involving lower symmetry and superstructure should inhibit complete solid solution and some intermediate composition might reasonably represent disordered metastable phases and/or sub-optical topotactic intergrowths.

Much attention has been devoted to the cation distribution in spinel-type oxides in the last decades (Lavina et al. 2002 and references therein), but only few crystal-chemical relationships are known for spinels containing Sb^{5+} or other pentavalent cations. According to Tarte and Rulmont (1988), the cation distribution over tetrahedral and octahedral sites in spinels containing high-valence cations is found to be in contradiction with the well known relative site preferences, which are based on their size and/or, in the case of cations subjected to Jahn-Teller distortion, on their crystal field stabilization energies.

To contribute to the scientific debate on the spinel crystal chemistry, we present the crystal structure determination of filipstadite from the type material (sample 163012, Smithsonian Institution, Washington, U.S.A.). Crystal chemical considerations led us to propose a tentative distribution of cations among octahedral and tetrahedral sites.

EXPERIMENTAL METHODS

X-ray diffraction

A crystal was selected and preliminarily examined with a Bruker P4 single-crystal diffractometer using graphite-monochromatized Mo*K*α radiation. The intensity data collection was done with an Oxford Diffraction Xcalibur 3 diffractometer, fitted with a Sapphire 2 CCD detector (see Table 1 for details). Intensity integration and standard Lorentz-polarization corrections were performed with the *CrysAlis* RED (Oxford Diffraction 2006) software package. The program ABSPACK in *CrysAlis* RED (Oxford Diffraction 2006) was used for the absorption correction. A total of 1754 frames of data were collected at room temperature

(2θ Mo$K\alpha$ < 64.60°) with an exposure time of 45 s per frame and a frame width of 0.90. All the 26652 reflections collected (1459 unique) yielded the cubic supercell: a = 25.9300(6) Å, V = 17434.4(5) Å^3, Z = 216 ($a = 3a_s$, with a_s = translation unit of a cubic spinel-type cell = 8.643 Å). No evidence of split of the superstructure reflections at high-theta angles was observed, thus suggesting no mixture with significant amounts of jacobsite [a = 8.4956(3) Å, Lucchesi et al. 1997; a = 8.3413(7) Å; Kim et al. 2009].

Electron microprobe analysis

The crystal used for the structural study was embedded in resin and polished for the chemical analysis that was performed using a CAMECA-CAMEBAX electron microprobe operating with a fine-focused beam (~ 1 μm) at an acceleration voltage of 20 kV and a beam current of 20 nA in wavelength-dispersive mode (WDS), with 10 s counting times for peak and 5 s for total background. X-ray counts were converted in oxide weight percentages using the PAP correction program supplied by CAMECA (Pouchou and Pichoir 1985). Standard, WDS line, analyzer crystal, and analytical uncertainty (wt%) for each element were the following: Mg (MgO, Mg$K\alpha$, TAP analyzer, 0.03); Al (Al_2O_3, Al$K\alpha$, TAP analyzer, 0.04); Si (diopside, Si$K\alpha$, TAP analyzer, 0.03); Mn ($MnTiO_3$, Mn$K\alpha$, LIF analyzer, 0.07); Fe (Fe_2O_3, Fe$K\alpha$, LIF analyzer, 0.11); Zn (ZnS, Zn$K\alpha$, LIF analyzer, 0.10); Sb (synthetic Sb_2S_3, Sb$L\alpha$, PET analyzer, 0.10). The crystal was found to be homogeneous without any inclusion of jacobsite.

Chemical formulae were calculated on the basis of four oxygen atoms and assuming that Mn and Fe are present at the divalent and trivalent state, respectively (Table 2). Sums of cations ranging from 2.996 to 3.010 apfu confirmed the above assumption.

STRUCTURE SOLUTION

The systematic absences in the whole intensity data set were consistent with the space group $Fd\bar{3}m$. Reflections were merged accordingly (R_{int} = 4.40%). The positions of metal atoms were found using the Patterson interpretation of the SHELXS-97 package (Sheldrick 2008); successive F_o-Fourier syntheses allowed us to locate all the O atoms yielding the expected unit-cell content. Full occupancy was assumed for all sites. Site-scattering values were refined for all cations using ionized atomic scattering factors as follows: Fe^{3+} vs. Mg^{2+} (T sites), Sb^{5+} vs. Mg^{2+} (M sites). The M1 octahedron resulted to be occupied by Sb^{5+} only and its occupancy was fixed accordingly. Both scattering curves and $\Delta f'$, $\Delta f''$ coefficients were taken from the *International Tables for X-ray Crystallography*, volume C (Wilson and Prince 1999). Anisotropic refinements by full-matrix least-squares on 110 refined parameters led to a final discrepancy factor of 4.41% for 681 observed reflections [$F_o > 4\sigma(F_o)$] and 6.40% for all unique 1459 data.

The mean electron numbers at the cation sites together with the atomic coordinates are reported in Table 3. Anisotropic displacement parameters are reported in Table 4. Table 5[1] lists the observed and calculated structure factors.

RESULTS

In keeping with the weakness of the superstructure reflections, the structure of filipstadite is topologically identical to the spinel-type structure with cations occupying 1/8 of the tetrahedral (T) and 1/2 of the octahedral (M) interstices of a cubic close-packing of oxygen atoms. Due to the cation ordering, the M and T sites of the spinel-type structure split into six and five independent sites, respectively. The structure of filipstadite, like that of common spinels, can be described as a sequence of pairs of polyhedral layers (hereafter

[1] For a copy of Table 5, document item AMxxxxx, contact the Business Office of the Mineralogical Society of America (see inside front cover of recent issue) for price information. Deposit items may also be available on the American Mineralogist web site at http://www.minsocam.org.

named X and Y) stacked along [111]. As far as the cation sites are concerned, X and Y layers have general formula M_3 and MT_2 respectively. As each layer is projected along [111], successive pairs of X-Y layers appear to be displaced ¼ $[11\bar{2}]$ with respect to each other. Thus, in the unit cell of spinels three identical XY pairs succeed along [111]. In filipstadite, the ordering of cations determines two types of M_3 layers, X and X′ (Fig.1, top), and two types of MT_2 layers, Y and Y′ (Fig. 1, bottom). The repeat unit, consisting of six polyhedral layers, namely X-Y-X′-Y′-X′-Y, is thus three times the XY unit of a basic spinel structure.

Taking into account the different multiplicity of both octahedral and tetrahedral cations (Table 3), the total electron number ($e^-_T + 2e^-_M = 25.0 + 53.6 = 78.6$) is in satisfactory accord with that (77.3) calculated on the basis of the chemical formula derived by microprobe data, $Mn^{2+}_{1.16}Mg_{0.83}Sb^{5+}_{0.50}Fe^{3+}_{0.48}Zn_{0.02}Al_{0.02}Si^{4+}_{0.01}O_4$. Bond distances and distortion parameters are reported in Table 6. All tetrahedra are rather regular and exhibit a small range of variation of the mean electron number (24.5 – 25.2), while the same value for the octahedral sites is very scattered (16.9 - 51.0). The overall average bond distances, weighted taking into account the different multiplicities of the individual sites, are 2.076 Å and 2.029 Å for octahedra and tetrahedra, respectively.

DISCUSSION

A site assignment in the structure of filipstadite is not straightforward and requires some reasonable simplifications. Minor cations were assigned to one site on the basis of their general site preference: in particular, Si^{4+} (Urusov 1983) and Zn (Navrotsky and Kleppa 1967) were assigned to the T site, and Al^{3+} (Urusov 1983) to the M site. Since electrons in M sites range from 16.9 up to 51.0, and in keeping with the literature on complex spinel-like antimonates (Tarte and Preudhomme 1979; Preudhomme et al. 1980; Tarte and Rulmont 1988), all Sb^{5+} was assigned to the M sites. On the other hand, the other main cations, i.e.

Mn^{2+}, Fe^{3+} and Mg, may occupy both the octahedral and the tetrahedral sites. Due to the fact that the relative preference for tetrahedral sites in spinels increases from Fe^{3+} and Mg towards Mn^{2+} (Hastings and Corliss 1956; Buessem and Butler 1963; Navrotsky and Kleppa 1967; Sawatzky et al. 1967; Morrish and Clark 1975; Lucchesi et al. 1997), one could be tempted to fill the T sites mainly with Mn^{2+} allowing all Fe^{3+} and Mg to occupy the M sites. The consequent assignment of all Fe^{3+} in the octahedra, indeed, would be in substantial accord with what observed in natural jacobsite, where Fe^{3+}, according to the Mössbauer study carried out by Maia et al. (1993), is ordered at the octahedral site. To evaluate the reliability of such a hypothesis, <M-O> distance was calculated with the remaining cations (2M = $Mg_{0.83}Mn^{2+}_{0.19}Fe^{3+}_{0.46}Al_{0.02}Sb^{5+}_{0.50}$) on the basis of pure <M-O> reference bond lengths (Table 7) and assuming a linear contribution of each cation. The value obtained (2.046 Å), markedly shorter than experimental one (2.076 Å), indicates that higher amounts of Mn^{2+}, the largest cation in filipstadite, enters the M sites and a mixing of Fe^{3+} and Mg enters the T sites. On the other hand, if all Fe^{3+} is located at the T sites together with Si and Zn and an appropriate mixing of Mn^{2+} and Mg to maintain the mean electron number close to 25, the <M-O> distance calculated with the remaining cations (2M = $Mg_{0.80}Mn^{2+}_{0.68}Al_{0.02}Sb^{5+}_{0.50}$) results even too long (2.087 Å) with respect to the observed mean value (2.076 Å), thus suggesting a more complex ordering model with Fe^{3+} entering both tetrahedral and octahedral cavities. Between the two arbitrary models described above, however, the second one leads to a minor discrepancy between the calculated and the observed value, indicating that Fe^{3+} is mainly located to tetrahedral sites; as a consequence, migration of higher than expected amounts of Mn^{2+} from tetrahedral into octahedral sites occurs, probably to balance the effects of the incorporation of the high-charged cation (Sb^{5+}) at the octahedra. Indeed, according to Tarte and Rulmont (1988), in spinel-like compounds containing “high valency cations” abnormal

cation distribution are observed which are unexpected on the basis of the well known preferences of cations for T and M sites.

In order to pursue a distribution of cations between T and M sites, the cation fractions obtained from chemical analysis were assigned taking into account the weighted electron number at both T and M sites, and minimizing the discrepancy between the calculated and the observed overall <M-O> distance. The overall <T-O> distance was not used as a constraint due to the well known differing of tetrahedral bond distances of the same cation as a function of the octahedral population (Lucchesi et al. 1998, 1999). On the contrary, it is known that tetrahedral cations show no or very minor influence on the octahedral M-O distances (Lavina et al. 2002). The following cation populations were obtained: 2M = 0.56 Mn^{2+} + 0.76 Mg + 0.16 Fe^{3+} + 0.02 Al + 0.50 Sb^{5+} (<n.e$^-$> = 53.0; $<M\text{-}O>_{calc}$ = 2.075 Å); T = 0.60 Mn^{2+} + 0.30Fe^{3+} + 0.07 Mg + 0.02 Zn + 0.01 Si (<n.e$^-$> = 24.4; $<T\text{-}O>_{calc}$ = 1.978 Å). As expected, for the tetrahedral distance the accord between observed and calculated values is not good; the calculated <T-O> distance remains too short (1.985 Å) even if a longer reference bond length for $^{IV}Mn^{2+}$-O (2.050 Å) is used as found by Hålenius et al. (2011) in the crystal structure of fully ordered galaxite ($MnAl_2O_4$). It must be taken into consideration, however, that the unusual presence of high-charged cations in the octahedra likely involves an overall lengthening of the tetrahedral distances. In this model, Fe^{3+} is disordered over tetrahedral and octahedral sites in a abundance ratio quite similar to that observed in the orthorhombic $M^{2+}{}_4Fe^{3+}SbO_8$ spinel-like compounds (M^{2+} = $Mg_{¾}Zn_{¼}$, Co, $Co_{¾}Ni_{¼}$, $Ni_{¾}Zn_{¼}$) where Fe^{3+} was proved to enter both T and M sites, in the 2:1 abundance ratio (Tarte and Preudhomme 1979).

Assuming as reliable the obtained partition between T and M sites, an attempt to assign cations among the individual sites was done as follows. In Figure 2, the <M-O> distances are plotted against the refined electron number together with data for pure reference bond lengths taken from literature (black circles) and, for a comparison, the sum of ionic radii of six-

coordinated cations and oxygen anions (empty triangles). Points fall along a line between M1 (the smallest octahedron occupied by Sb alone) and M4, the largest (2.117 Å) octahedron dominated by Mg ($n.e^- = 16.9$). Its position on the plot falls on the Mg-Mn^{2+} join, suggesting incorporation of only Mn^{2+} replacing for Mg. After the M4 assignment, the remaining octahedral cations (i.e., 0.48 Mg + 0.40 Mn^{2+} + 0.16 Fe^{3+} + 0.02 Al) were tentatively considered as an unique 'mixed' ME species (empty square in Fig. 2) having $<n.e^->$ = 19.0 and $<ME\text{-}O>_{calc}$ = 2.111 Å. Since the data relative to M5, M6, M3, and M2 show an alignment without significant displacements from the ME-M1 segment, it was made the assumption that the given above 'mixed' ME species replaces Sb^{5+} at different degrees without any preference for different octahedral sites. Thus, a mixed population [ME_x Sb^{5+}_{1-x}] with x = 0.903, 0.781, 0.744, and 0.424, was assigned to M5, M6, M3 and M2, respectively. To check the reliability of this hypothesis, we compared the observed <M-O> distances to those calculated on the basis of the pure <M-O> reference bond lengths (Table 7). The calculated distances match fairly well the observed values (Fig. 3). The cation populations thus obtained are given in Table 8.

Due to the relative homogeneity in the mean electron number at the tetrahedral sites (24.5 – 25.2), it is rather difficult to derive a reliable cation distribution of the remaining 0.60 Mn^{2+} + 0.30Fe^{3+} + 0.07 Mg + 0.02 Zn + 0.01 Si among the five tetrahedral sites on the basis of the mean distances alone (Fig. 4), being the geometrical features of tetrahedra in spinels strongly depending on the octahedral cation population, especially in this case, where the high-charge Sb^{5+} cation heavily affects the bond strengths on the oxygen atoms. In the structure of filipstadite, like in the spinel structure, each oxygen atom adopts a tetrahedral configuration linking three M cations and one T. In Figure 5 the individual tetrahedral T-O_i distances are plotted against the sum of the positive charge in the three M cations linked to each O_i. Obviously, the site fully occupied by Sb^{5+} (M1) overcharges the linked O5 oxygen

atoms; as a consequence, T2-O5 is the longest individual T-O_i in the structure (2.079 Å) whereas the O10 oxygen atom, which is bonded to three M4 (occupied by divalent cations alone) and one T3, links T3 with the shortest individual T-O_i distance (1.873 Å). The charge distribution at the octahedral sites surely affects the partition of Fe^{3+} and divalent cations (mainly Mn^{2+} and minor amounts of Mg) among the tetrahedra. The smallest and most regular T3 tetrahedron, located within the Y layer, is surrounded by twelve M4 octahedra (yellow in Fig. 1: six belonging to the overlying X, three to Y, and three to the underlying X′ layer) and should be assumed as occupied dominantly by Fe^{3+} and Si. On the other hand, T2 shows the longest <T-O> distance (2.068 Å), even longer than the pure <Mn^{2+}-O> reference distance (2.036 Å). To this site, which exhibits a mean electron number slightly higher than 25, the available Zn was assigned together with Mn^{2+}. To the other tetrahedral sites, namely T5 (2.030 Å), T4 (1.992 Å) and T1 (1.989 Å) the remaining Mn^{2+}, Mg and Fe^{3+} were tentatively assigned taking into account both the mean bond distances and the electron number (Table 8). Although the discrepancies between calculated and observed values for tetrahedral bond distances are rather high and the observed values, as expected, are higher than those calculated on the basis of pure reference bond lengths (Fig. 6), the bond strength sums on oxygen atoms calculated using the assigned cation populations are indeed quite satisfactory (Table 9).

ACKNOWLEDGEMENTS

Authors thank Pete Dunn who provided us with a crystal from the type material (sample 163012, Smithsonian Institution, Washington, U.S.A.). Thanks are also due to Fabrizio Nestola (University of Padova) for the chemical analyses. The manuscript benefited from the revision of two anonymous reviewers. This work was funded by "Progetto d'Ateneo

249 2009" and M.I.U.R., P.R.I.N. 2009 project "Modularity, microstructures and non-
250 stoichiometry in minerals".

251

252 REFERENCES

253 Brese, N.E. and O'Keeffe, M. (1991) Bond-valence parameters for solids. Acta
254 Crystallographica, B47, 192-197.

255 Buessem, W.R. and Butler, S.R. (1963) Valence Changes of Iron and Manganese in
256 Manganese Ferrite. Journal of the American Ceramic Society, 46, 442-446.

257 Dunn, P.J., Peacor, D.R., Criddle, A.J. and Stanley, C.J. (1988) Filipstadite, a new Mn-Fe^{3+}-
258 Sb derivative of spinel, from Långban, Sweden. American Mineralogist, 73, 413-419.

259 Hålenius, U., Bosi, F. and Skogby, H. (2011) A first record of strong structural relaxation of
260 TO_4 tetrahedra in a spinel solid solution. American Mineralogist, 96, 617-622.

261 Hastings, J.M. and Corliss, L.M. (1956) Neutron Diffraction Study of Manganese Ferrite.
262 Physical Review, 104, 328-331.

263 Holtstam, D. (1993) A second occurrence of filipstadite in Värmland, Sweden. Geologiska
264 Föreningens i Stockholm Förhandlingar, 115, 239-240.

265 Holtstam, D. and Larsson, A.-K. (2000) Tegengrenite, a new, rhombohedral spinel-related Sb
266 mineral from the Jakobsberg Fe-Mn deposit, Värmland, Sweden. American
267 Mineralogist, 85, 1315-1320.

268 Holtstam, D., Nysten, P., and Gatedal, K. (1998) Parageneses and compositional variations of
269 Sb oxyminerals from Långban-type deposits in Värmland, Sweden. Mineralogical
270 Magazine, 62, 395-407.

271 Kim, J.G., Seo, J.W., Cheon, J. and Kim, Y.J. (2009) Rietveld Analysis of Nano-crystalline
272 $MnFe_2O_4$ with Electron Powder Diffraction. Bulletin of Korean Chemical Society, 30,
273 183-187.

Ibers, J.A. and Hamilton, W.C. Eds. (1974) International Tables for X-ray Crystallography, vol. IV, 366p. Kynock, Dordrecht, The Netherlands.

Lavina, B., Salviulo, G. Della Giusta A. (2002) Cation distribution and structure modelling of spinel solid solutions. Physics and Chemistry of Minerals, 29, 10-18.

Lucchesi, S., Della Giusta, A. and Russo, U. (1998) Cation distribution in natural Zn-aluminate spinels. Mineralogical Magazine, 62, 41-54.

Lucchesi, S., Russo, U. and Della Giusta, A. (1997) Crystal chemistry and cation distribution in some Mn-rich natural and synthetic spinels. European Journal of Mineralogy, 9, 31-42.

Lucchesi, S., Russo, U. and Della Giusta, A. (1999) Cation distribution in natural Zn-spinels: franklinite. European Journal of Mineralogy, 11, 501-511.

Maia, H.A., De Araujo, F.F.T., De Araujo, M.A.B., Danon, J. and Frankel, R.B. (1993) Cation distribution in natural ferrites. Hyperfine Interactions, 77, 43-50.

Morrish, A.H. and Clark, P.E. (1975) High-field M6ssbauer study of Mn-Zn ferrites. Physical Review B, 11, 278-286.

Navrotsky, A. and Kleppa, O.J. (1967) The thermodynamics of cation distribution in simple spinels. Journal of Inorganic and Nuclear Chemistry, 29, 2701-2714.

Oxford Diffraction (2006). CrysAlis RED (Version 1.171.31.2) and ABSPACK in CrysAlis RED. Oxford Diffraction Ltd, Abingdon, Oxfordshire, England.

Pouchou, J.L. and Pichoir, F. (1985) PAP correction procedure for improved microanalysis. In: J.T. Armstrong (Ed.), Microbeam Analysis. San Francisco Press, San Francisco, pp. 104-106.

Preudhomme, J., Tarte, P., Kenens, K., Grandjean, F. and Gerard, A. (1980) Studies of spinels. VIII. Synthesis and structural study of new antimonates $M^{II}_5M^{III}_3SbO_{12}$ by X-

ray diffraction and Mössbauer spectroscopy. Académie Royale de Belgique, Bulletin de la Classe des Sciences, 66, 776-791.

Robinson, K., Gibbs, G.V. and Ribbe, P.H. (1971) Quadratic elongation; a quantitative measure of distortion in coordination polyhedra. Science, 172, 567-570.

Sawatzky, G.A., van der Wonde, F. and Morrish, A.H. (1967) Note on cation distribution of $MnFe_2O_4$. Physics Letters, A, 25, 147-148.

Sheldrick, G.M. (2008) A short history of SHELX. Acta Crystallographica, A64, 112-122.

Tarte, P. and Preudhomme, J. (1979) Studies of spinels. VI. Antimonates $M^{II}_4M^{III}Sb^{V}O_8$, a new, large family of spinels presenting order-disorder transitions. Journal of Solid State Chemistry, 29, 273-284.

Tarte, P. and Rulmont, A. (1988) Factors determining the cation distribution in spinels: the case of spinels containing several high-valency cations. Journal of Materials Science Letters, 7, 551-554.

Urusov, S.V. (1983) Interaction of cations on octahedral and tetrahedral sites in simple spinels. Physics and Chemistry of Minerals, 9, 1-5.

Wilson, A. J. C. and Prince, E., Eds. (1999) *International Tables for X-ray Crystallography*, Volume C: Mathematical, physical and chemical tables (2nd Edition), Kluwer Academic, Dordrecht, NL.

FIGURE CAPTIONS

FIGURE 1_ Polyhedral layers in the structure of filipstadite projected along [111]. Octahedra are pictured with different colors as a function of the electron number obtained by occupancy refinement: < 20 = yellow (M4), 20 ÷ 30 = orange (M3, M5, M6); 30 ÷ 40 = red (M2); > 40 = dark red (M1). All tetrahedra are in gray. Along [111] the

repeat unit consists of six polyhedral layers, namely X-Y-X′-Y′-X′-Y. Successive slab of six layers are displaced ¼ [11 $\bar{2}$] with respect to each other.

FIGURE 2_ The octahedral <M-O> distances plotted against the refined electron number in the M sites of filipstadite (black squares); black circles refer to data for reference bond lengths taken from literature (see Table 7) and empty triangles refer to the sum of ionic radii of six-coordinated cations and oxygen anions. The empty square (<n.e$^-$> = 19.0 and <ME-O>$_{calc}$ = 2.111 Å) represents a 'mixed' species ME = 45% Mg + 38% Mn^{2+} + 15% Fe^{3+} + 2% Al. Dashed lines mark the Mg-Mn^{2+} and ME-M1 joins.

FIGURE 3_ <M-O> distances calculated on the basis of the proposed cation distribution among octahedral sites plotted against the observed values. The <M1-O> distance (1.958 Å) was used as pure <Sb^{5+}-O>. Dashed line refers to y = x line. Data fit the following linear regression <M-O>$_{calc}$ = 1.04(5) <M-O>$_{obs}$ + 0.1(1), r^2 = 0.987]. The <M1-O> distance (empty square) was not included in the linear model.

FIGURE 4_ The tetrahedral <T-O> distances plotted against the refined electron number in the T sites of filipstadite (black squares); black circles refer to data for reference bond lengths taken from literature (see Table 7) and empty triangles refer to the sum of ionic radii of four-coordinated cations and oxygen anions.

FIGURE 5_ Individual T-O_i distances plotted against the sum of cation charge in the three M sites bonded to each O_i.

FIGURE 6_ <T-O> distances calculated on the basis of the proposed cation distribution among tetrahedral sites plotted against the observed values. Dashed line refers to y = x line. Data fit the following linear regression $<T\text{-}O>_{calc}$ = 1.0(3)$<T\text{-}O>_{obs}$ - 0.0(6), r^2 = 0.74.

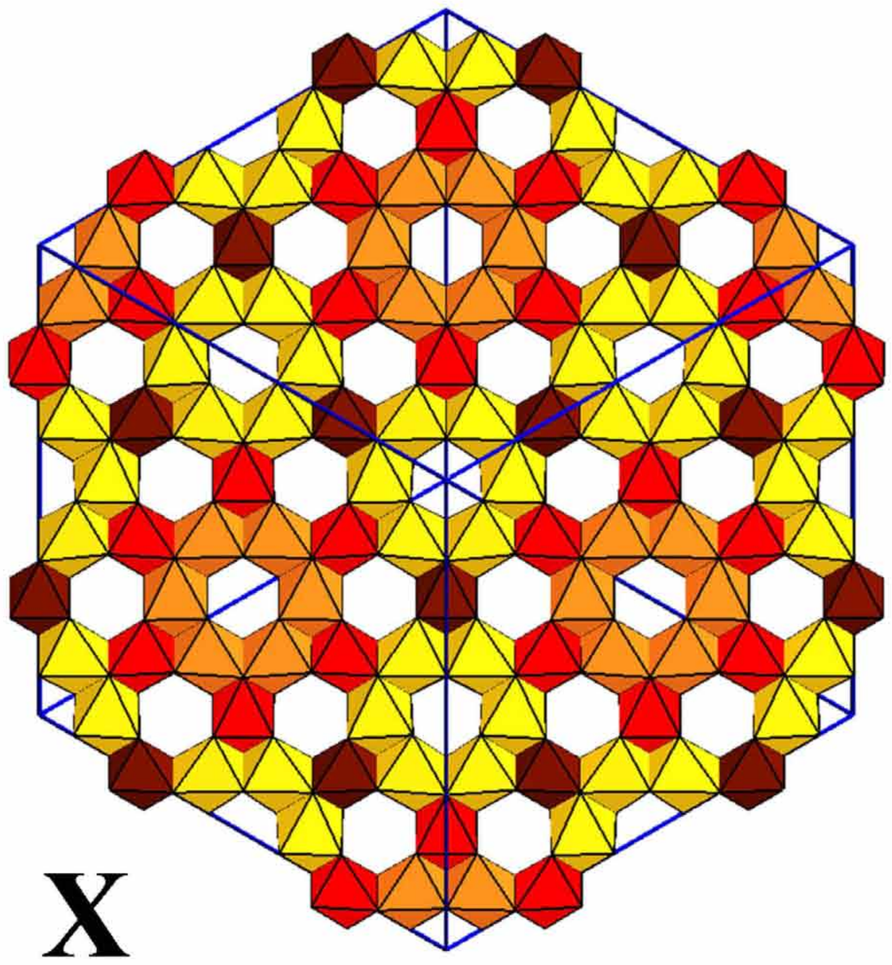

X

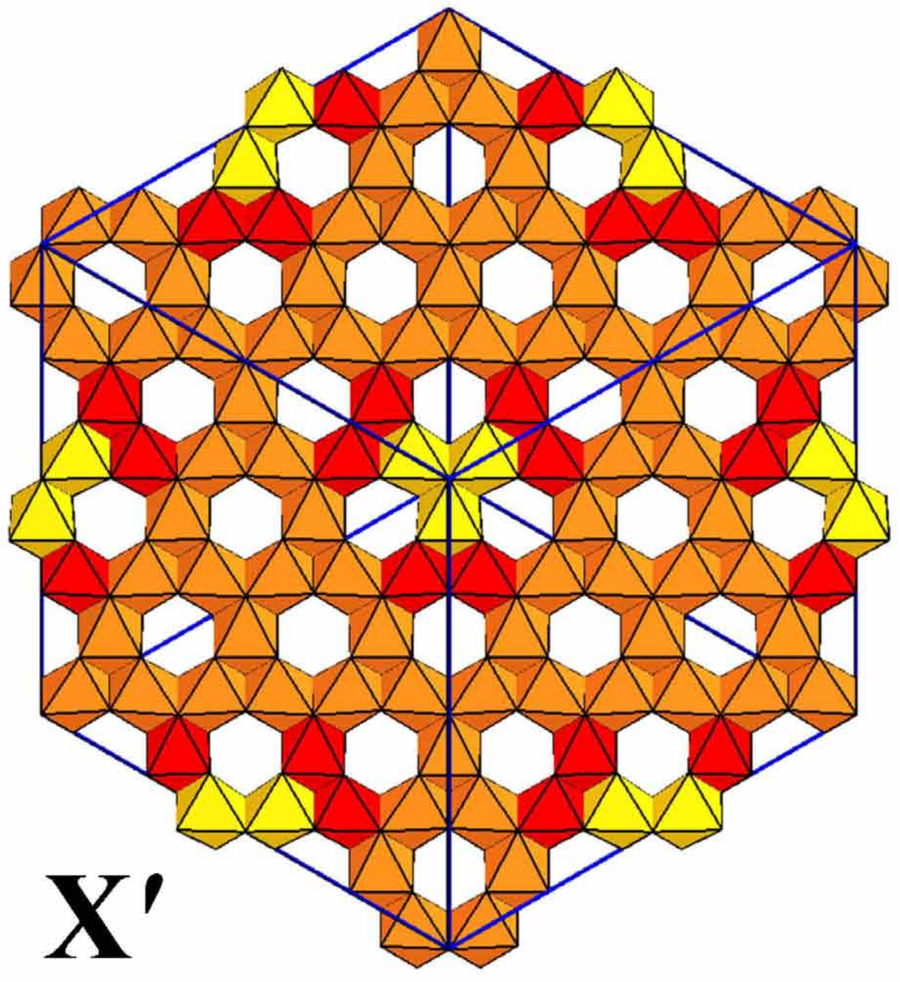

X′

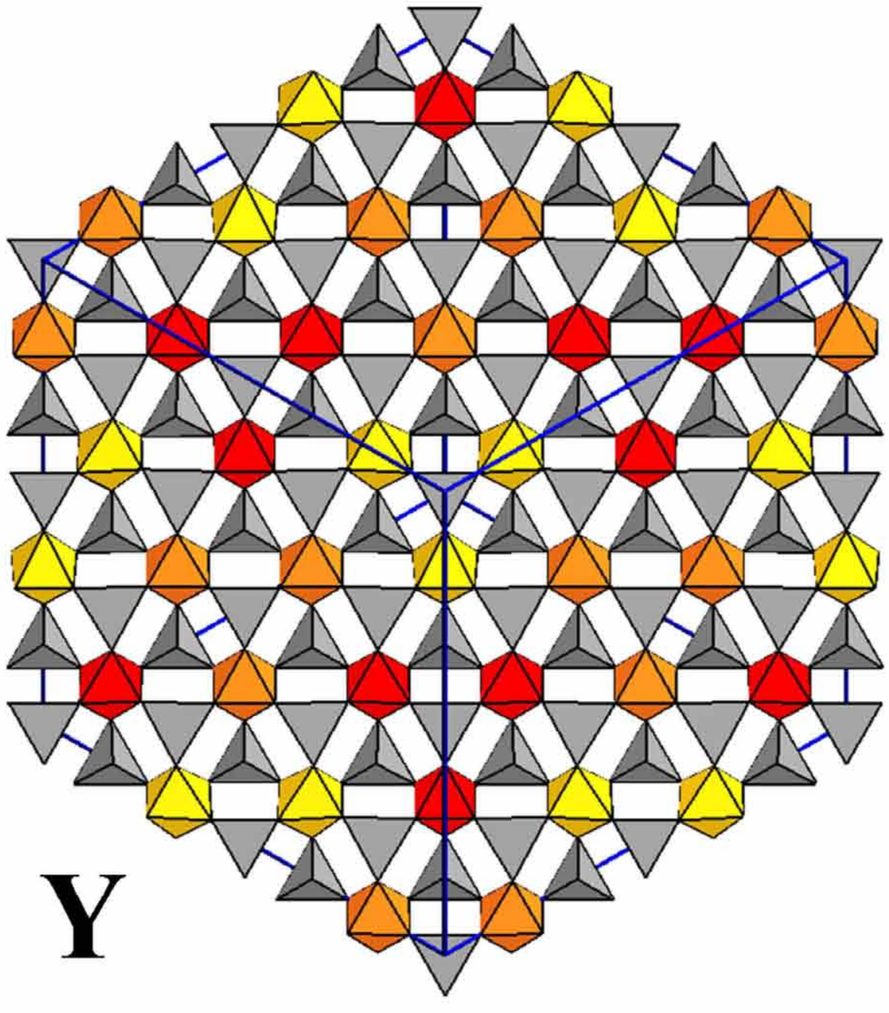

Y

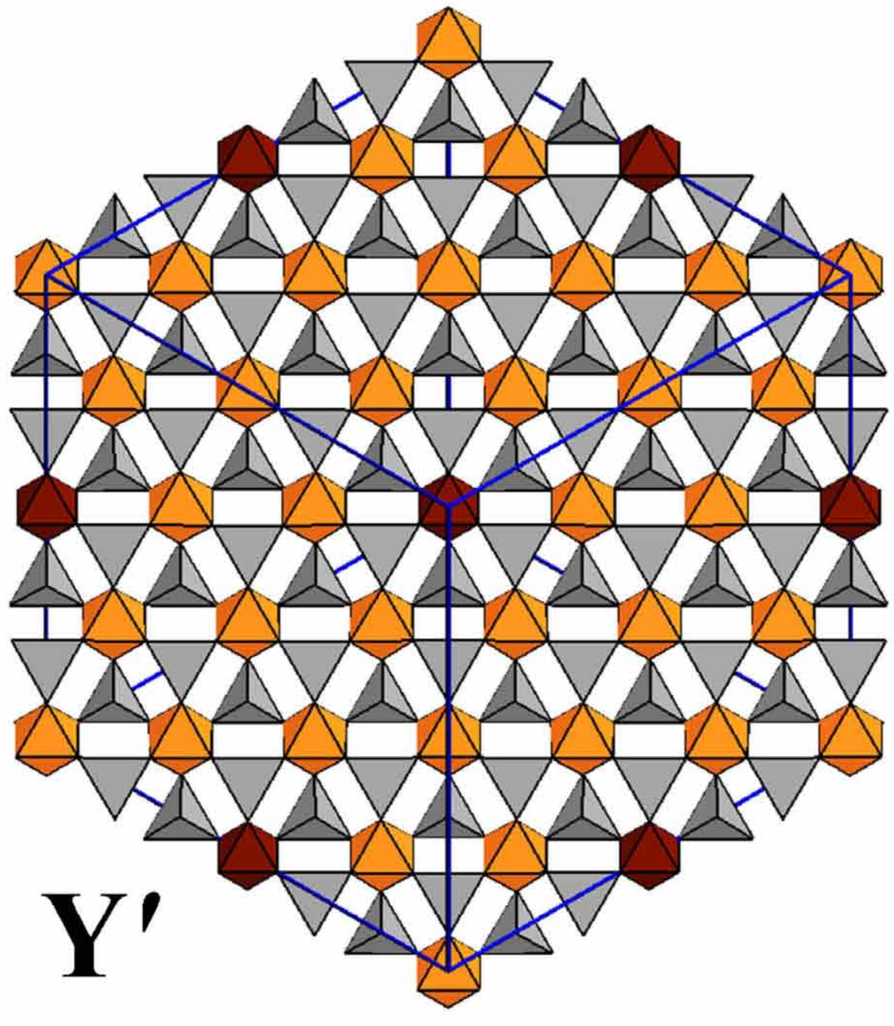

Y′

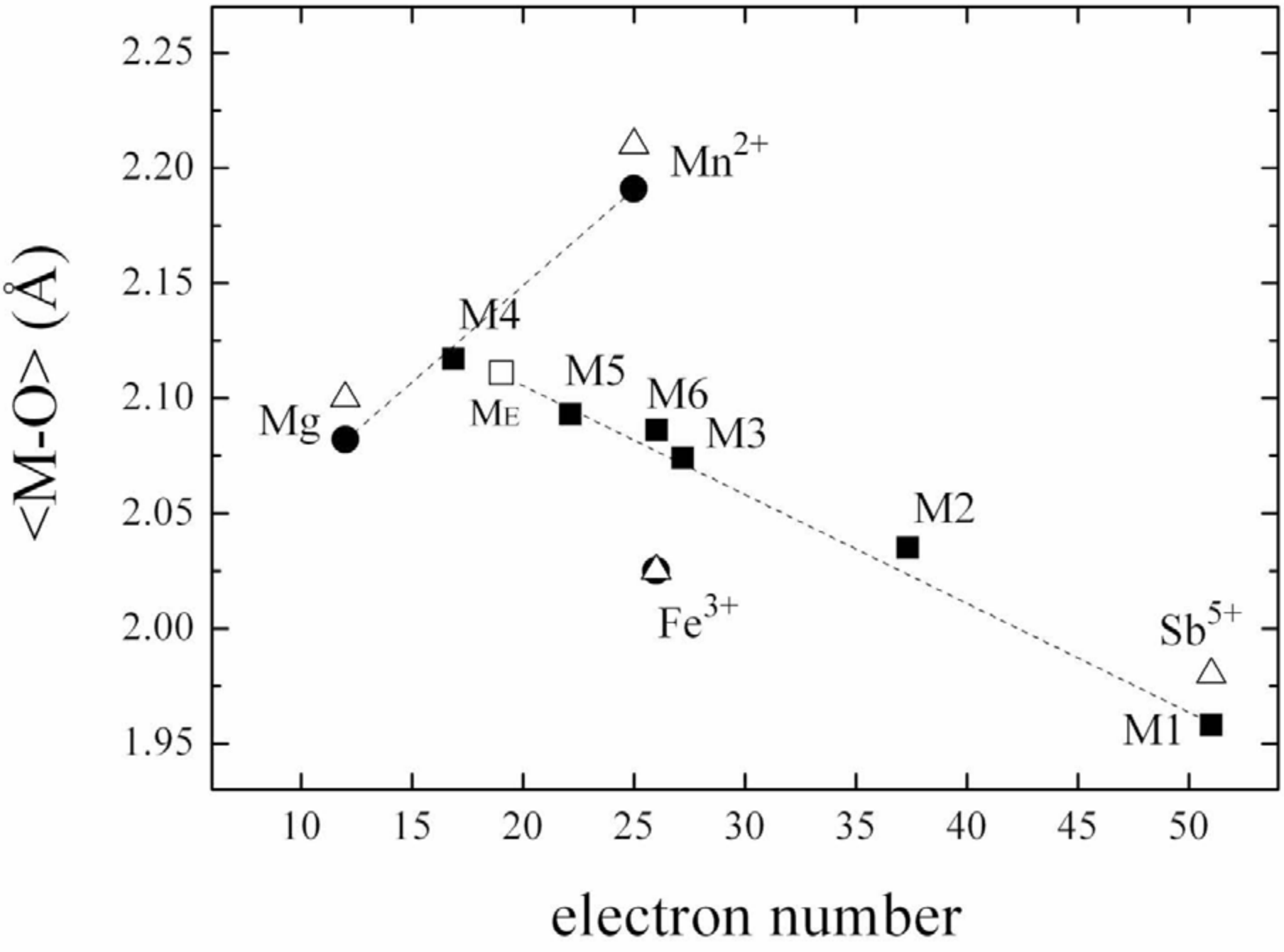
2.25
2.20
2.15
2.10
2.05
2.00
1.95
<M-O> (Å)
10
15
20
25
30
35
40
45
50
electron number
Mn2+
M4
M5
M6
M3
M2
ME
Mg
Fe3+
Sb5+
M1

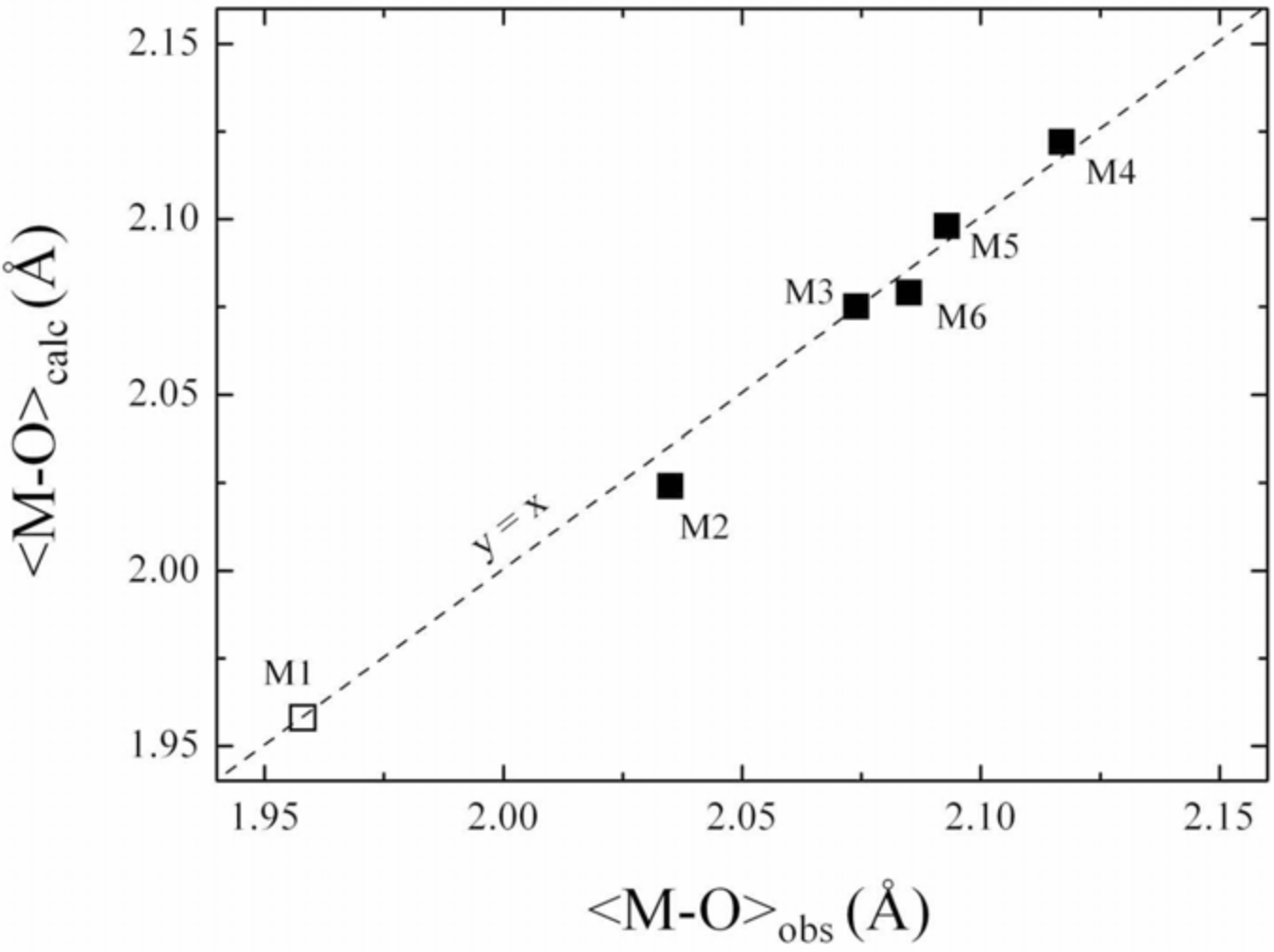
2.15
2.10
2.05
2.00
1.95
1.95
2.00
2.05
2.10
2.15
<M-O>calc (Å)
<M-O>obs (Å)
y = x
M1
M2
M3
M4
M5
M6

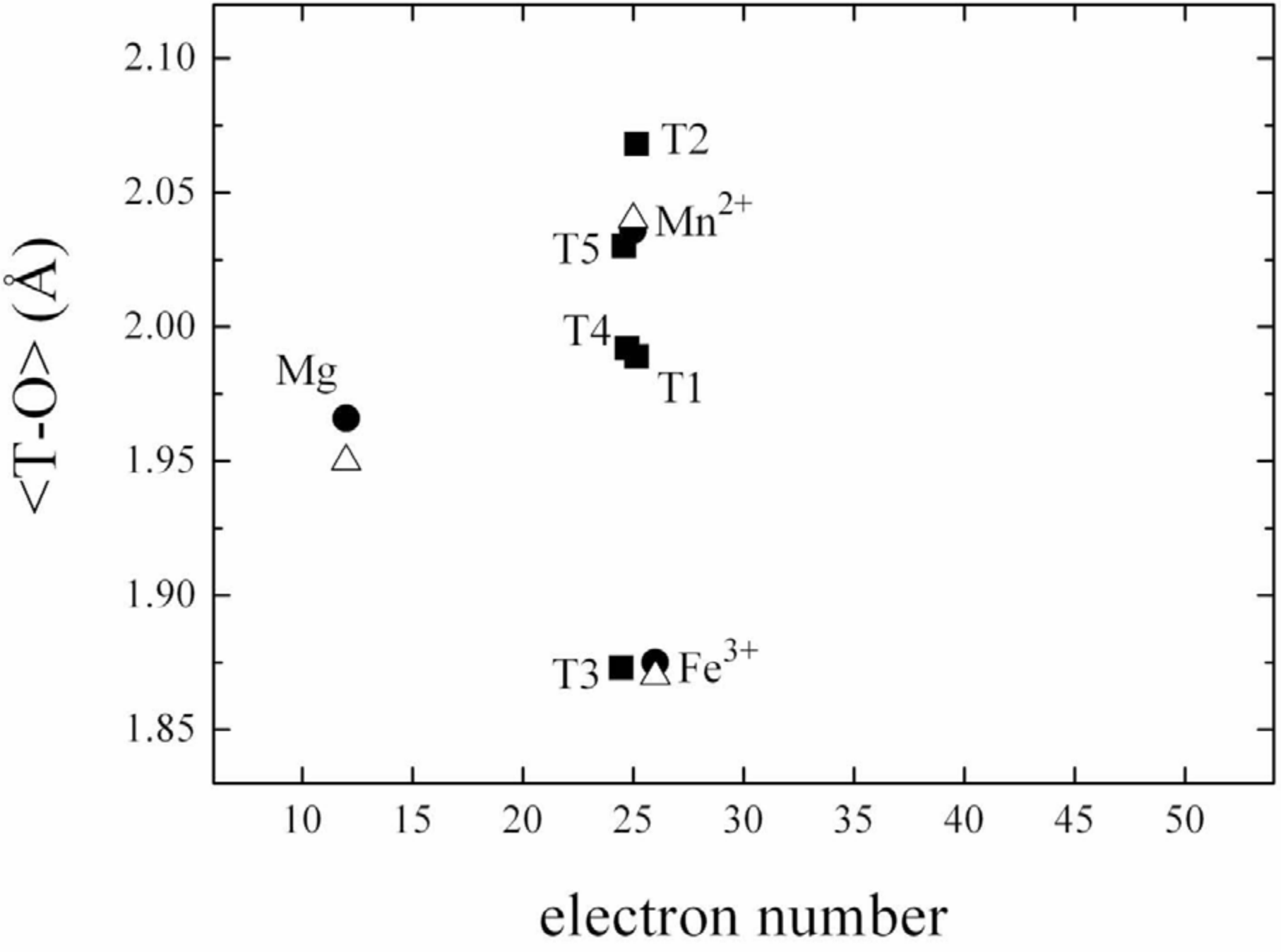
2.10
2.05
2.00
1.95
1.90
1.85
<T-O> (Å)
10
15
20
25
30
35
40
45
50
electron number
T2
Mn2+
T5
T4
T1
Mg
T3
Fe3+

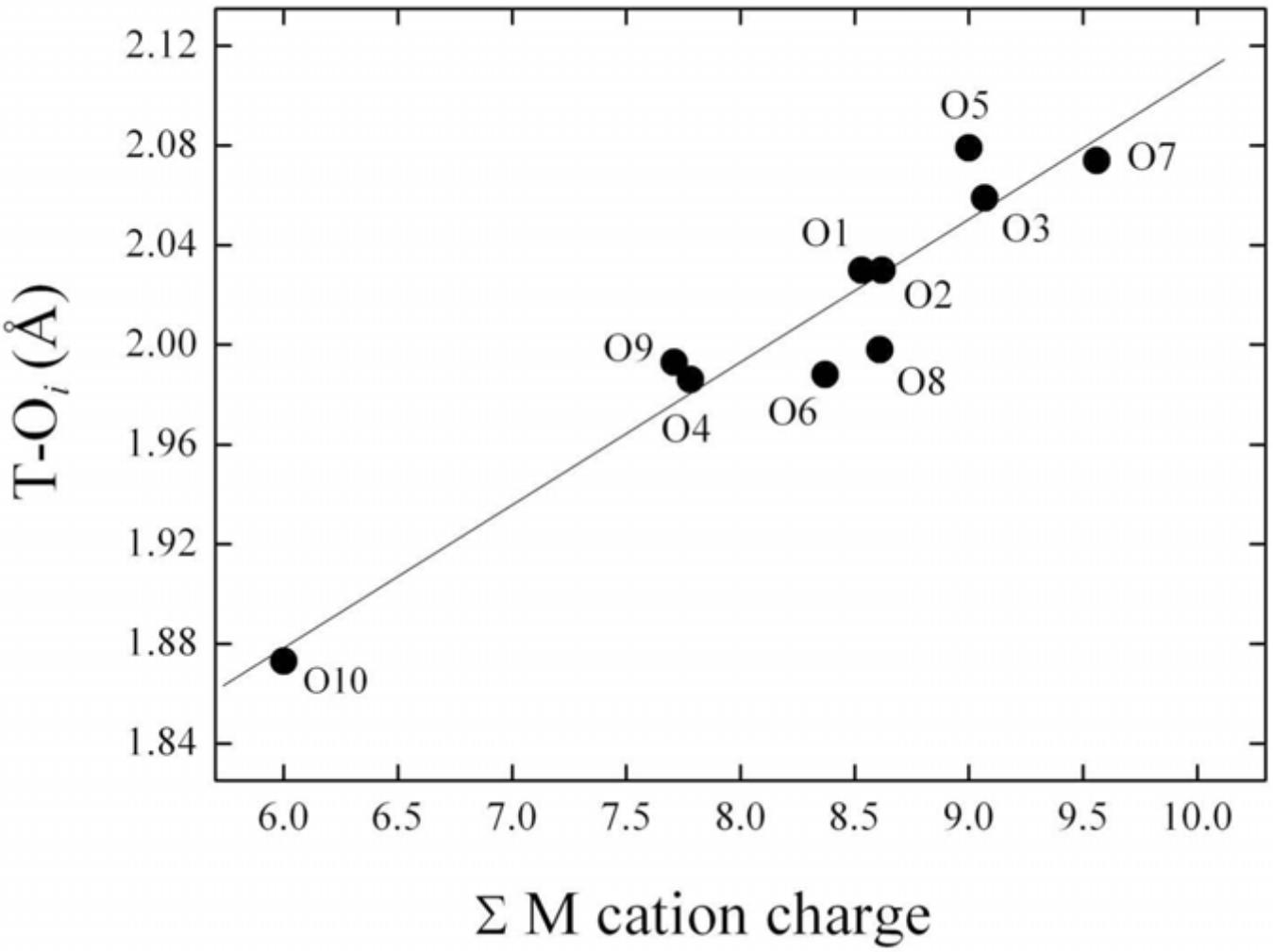
2.12
2.08
2.04
2.00
1.96
1.92
1.88
1.84
T-O$_i$ (Å)
6.0
6.5
7.0
7.5
8.0
8.5
9.0
9.5
10.0
Σ M cation charge
O5
O7
O3
O1
O2
O9
O8
O6
O4
O10

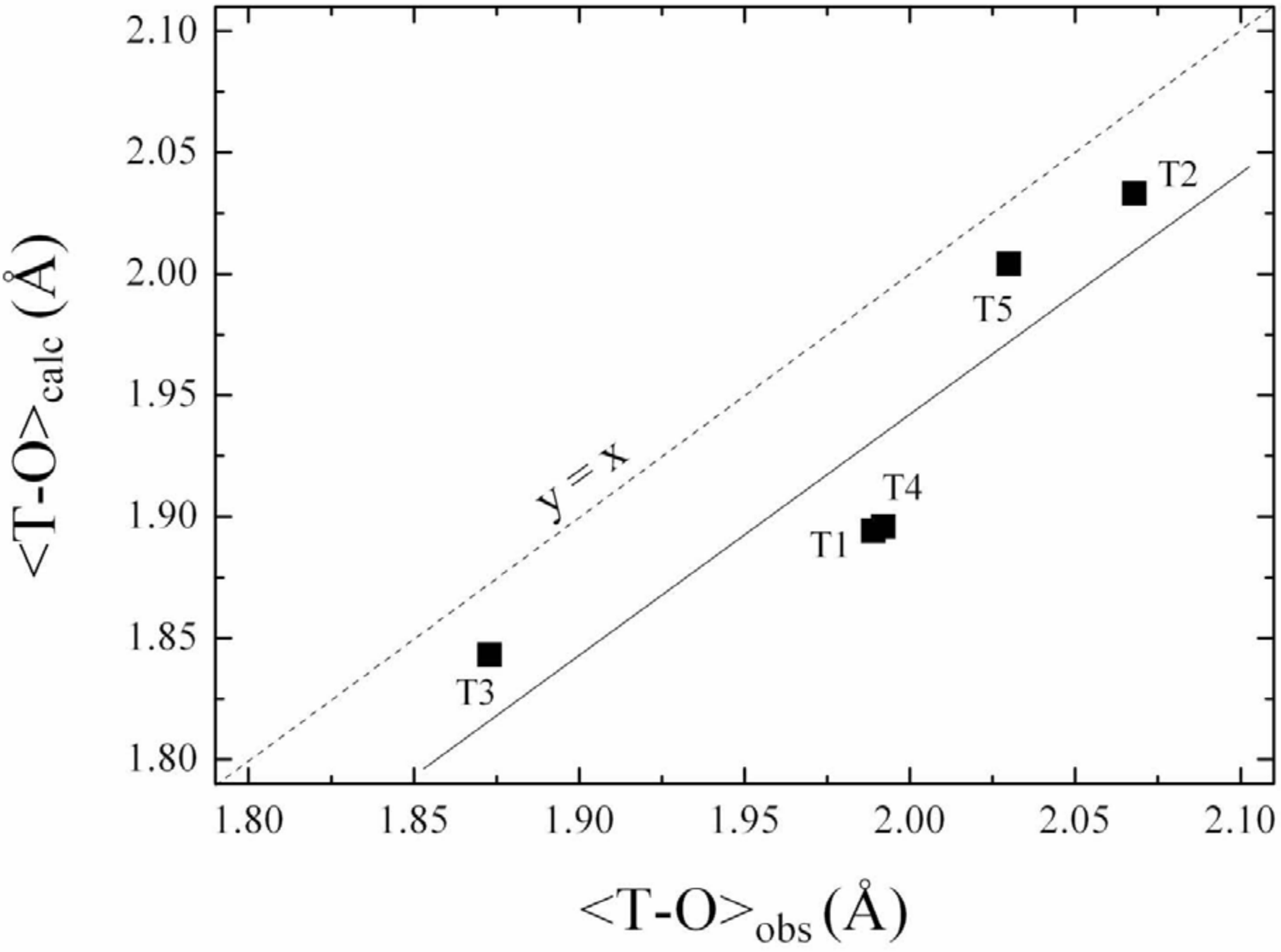
2.10
2.05
2.00
1.95
1.90
1.85
1.80
<T-O>calc (Å)
y = x
T2
T5
T4
T1
T3
1.80
1.85
1.90
1.95
2.00
2.05
2.10
<T-O>obs (Å)

TABLE 1 – Crystallographic data and refinement parameters for filipstadite

Crystal data	
Ideal formula	$(Mn^{2+},Mg)_2(Sb,Fe^{3+})O_4$
Crystal system	Cubic
Space group	$Fd\bar{3}m$ (origin #2)
Unit-cell parameters a, c (Å)	25.9300(6)
Unit-cell volume (Å^3)	17434.4(7)
Z	216
Crystal size (mm)	0.055×0.060×0.065
Data collection	
Diffractometer	Oxford Diffraction Xcalibur 3
Temperature (K)	298(3)
Radiation, wavelength (Å)	$Mo_{K\alpha}$, 0.71073
θ_{max} for data collection (º)	32.30
h, k, l ranges	-38 ÷ 37, -37 ÷ 20, -30 ÷ 35
Detector to sample distance (cm)	5
Number of frames	1754
Measuring time/frame (s)	45
Frame width (°)	0.90
Total reflections collected	26652
Unique reflections (R_{int})	1459 (4.40%)
Unique reflections $F > 4\sigma(F)$	681
Absorption correction method	ABSPACK (Oxford Diffraction 2006)
Structure refinement	
Refinement method	Full-matrix least-squares on F^2
Weighting scheme	$1/\sigma^2(F)$
Data/restraints/parameters	1459/0/110
R_1 [$F > 4\sigma(F)$]	4.41%
R_1 all	6.42%
Largest diff. peak and hole (e$^-$/Å^3)	1.17, -1.45

TABLE 2 – Electron microprobe analyses (wt % of oxides) and atomic ratios (on the basis of 4 oxygen atoms) for the selected filipstadite crystal.

	1	2	3	4	5	mean
Sb_2O_5	33.61	33.85	33.77	33.31	33.74	33.66
SiO_2	0.31	0.28	0.33	0.27	0.28	0.29
Fe_2O_3	15.56	15.14	15.27	15.60	15.52	15.42
Al_2O_3	0.50	0.55	0.49	0.54	0.57	0.53
ZnO	0.58	0.62	0.62	0.69	0.57	0.62
MnO	34.19	34.51	34.99	34.71	34.81	34.64
MgO	13.86	14.05	14.45	13.77	13.84	13.99
Total	98.50	99.00	99.90	98.88	99.33	99.15
Sb	0.498	0.500	0.493	0.493	0.497	0.496
Si	0.012	0.011	0.013	0.011	0.011	0.012
Fe^{3+}	0.467	0.453	0.452	0.467	0.463	0.460
Al	0.023	0.026	0.023	0.025	0.027	0.025
Zn	0.017	0.018	0.018	0.020	0.017	0.018
Mn^{2+}	1.155	1.161	1.165	1.170	1.168	1.164
Mg	0.824	0.832	0.847	0.817	0.817	0.827
$\Sigma_{cations}$	2.996	3.000	3.010	3.004	2.999	3.002

Notes: Mn and Fe were assumed as divalent and trivalent, respectively

TABLE 3 – Fractional atomic coordinates and equivalent isotropic displacement parameters (Å^2)

	Wyckoff	occupancy	x	y	z	U_{eq}
M1	16*d*	$Sb_{1.000}$	1/2	1/2	1/2	0.0191(3)
M2	96*g*	$Sb_{0.65(2)}Mg_{0.35}$	−0.08317(2)	−0.08317(2)	0.16703(2)	0.0209(3)
M3	96*g*	$Sb_{0.39(1)}Mg_{0.61}$	0.00019(2)	0.00019(2)	0.16626(3)	0.0223(4)
M4	96*g*	$Sb_{0.125(8)}Mg_{0.875}$	0.08548(4)	0.08548(4)	0.50417(6)	0.0255(7)
M5	96*g*	$Sb_{0.26(1)}Mg_{0.74}$	0	0.08217(3)	−0.08217(3)	0.0234(5)
M6	32*e*	$Sb_{0.36(1)}Mg_{0.64}$	0.16674(3)	0.16674(3)	0.16674(3)	0.0217(5)
T1	32*e*	$Fe_{0.94(4)}Mg_{0.06}$	0.29109(4)	0.29109(4)	0.29109(4)	0.0240(7)
T2	96*g*	$Fe_{0.94(3)}Mg_{0.06}$	0.04165(3)	0.04165(3)	0.37540(4)	0.0235(5)
T3	8*b*	$Fe_{0.89(5)}Mg_{0.11}$	3/8	3/8	3/8	0.022(1)
T4	32*e*	$Fe_{0.91(4)}Mg_{0.09}$	0.04204(4)	0.04204(4)	0.04204(4)	0.0217(7)
T5	48*f*	$Fe_{0.90(3)}Mg_{0.10}$	0.95808(5)	1/8	1/8	0.0185(6)
O1	96*g*		0.0797(2)	0.0797(2)	0.2469(2)	0.023(1)
O2	96*g*		−0.0805(2)	−0.0805(2)	0.0885(2)	0.025(1)
O3	192*i*		0.1633(1)	−0.0051(2)	−0.0797(1)	0.024(1)
O4	96*g*		−0.0847(1)	−0.0847(1)	0.2457(2)	0.023(1)
O5	96*g*		0.0031(1)	0.0031(1)	0.5754(2)	0.021(1)
O6	32*e*		0.0863(2)	0.0863(2)	0.0863(2)	0.027(2)
O7	96*g*		0.0885(2)	0.0885(2)	0.4202(2)	0.022(1)
O8	32*e*		0.2466(2)	0.2466(2)	0.2466(2)	0.023(2)
O9	96*g*		−0.0023(2)	−0.0023(2)	0.0865(2)	0.027(1)
O10	32*e*		0.4167(2)	0.4167(2)	0.4167(2)	0.026(2)

TABLE 4 – Anisotropic displacement parameters (Å^2) for atoms in filipstadite

	U_{11}	U_{22}	U_{33}	U_{23}	U_{13}	U_{12}
M1	0.0191(3)	0.0191(3)	0.0191(3)	-0.0004(2)	-0.0004(2)	-0.0004(2)
M2	0.0204(3)	0.0204(3)	0.0219(3)	0.0014(1)	0.0014(1)	-0.0002(2)
M3	0.0223(4)	0.0223(4)	0.0222(5)	-0.0024(2)	-0.0024(2)	-0.0008(3)
M4	0.0278(8)	0.0278(8)	0.0210(9)	-0.0010(4)	-0.0010(4)	-0.0071(6)
M5	0.0235(7)	0.0234(5)	0.0234(5)	-0.0028(4)	0.0021(3)	0.0021(3)
M6	0.0217(5)	0.0217(5)	0.0217(5)	-0.0022(3)	-0.0022(3)	-0.0022(3)
T1	0.0240(7)	0.0240(7)	0.0240(7)	-0.0003(3)	-0.0003(3)	-0.0003(3)
T2	0.0237(6)	0.0237(6)	0.0230(7)	-0.0011(3)	-0.0011(3)	0.0011(3)
T3	0.022(1)	0.022(1)	0.022(1)	0	0	0
T4	0.0217(7)	0.0217(7)	0.0217(7)	-0.0001(3)	-0.0001(3)	-0.0001(3)
T5	0.0181(7)	0.0186(6)	0.0186(6)	0.0014(4)	0	0
O1	0.024(2)	0.024(2)	0.021(2)	0.002(1)	0.002(1)	0.011(2)
O2	0.026(2)	0.026(2)	0.023(2)	0.003(1)	0.003(1)	0.004(2)
O3	0.024(2)	0.023(2)	0.026(2)	-0.006(1)	-0.005(1)	0.001(1)
O4	0.022(2)	0.022(2)	0.024(2)	0.007(1)	0.007(1)	0.005(2)
O5	0.023(1)	0.023(1)	0.015(2)	0.001(1)	0.001(1)	0.006(2)
O6	0.027(2)	0.027(2)	0.027(2)	0.005(2)	0.005(2)	0.005(2)
O7	0.021(1)	0.021(1)	0.024(2)	0.005(1)	0.005(1)	0.002(2)
O8	0.023(2)	0.023(2)	0.023(2)	0.003(2)	0.003(2)	0.003(2)
O9	0.029(2)	0.029(2)	0.025(2)	-0.009(1)	-0.009(1)	0.005(2)
O10	0.026(2)	0.026(2)	0.026(2)	-0.001(2)	-0.001(2)	-0.001(2)

TABLE 6 – Selected bond distances (Å) for filipstadite

M1- O5(x6)	1.958(5)	M2- O3(x2)	2.029(4)	M3- O1(x2)	2.066(4)
mean	1.958	O7(x2)	2.037(3)	O9	2.070(5)
V	9.92	O2	2.039(5)	O3(x2)	2.078(4)
σ^2	25.11	O4	2.041(5)	O8	2.087(5)
λ	1.0067	*mean*	2.035	*mean*	2.074
		V	11.11	*V*	11.75
		σ^2	28.46	σ^2	29.39
		λ	1.0077	λ	1.0079
M4- O10	2.053(5)	M5- O9(x2)	2.075(4)	M6- O1(x3)	2.083(5)
O4(x2)	2.081(4)	O2(x2)	2.094(4)	O6(x3)	2.089(5)
O5(x2)	2.152(4)	O3(x2)	2.109(4)	*mean*	2.086
O7	2.180(5)	*mean*	2.093	*V*	11.98
mean	2.117	*V*	12.05	σ^2	2518
V	12.39	σ^2	34.30	λ	1.0067
σ^2	48.03	λ	1.0093		
λ	1.0141				
T1- O4(x3)	1.986(6)	T2- O3(x2)	2.059(5)	T3- O10(x4)	1.873(9)
O8	1.998(9)	O7	2.074(6)	*mean*	1.873
		O5	2.079(5)	*V*	3.37
mean	1.989	*mean*	2.068		
V	4.03	*V*	4.53		
σ^2	1.39	σ^2	0.50		
λ	1.0003	λ	1.0001		
T4- O6	1.988(9)	T5- O1(x2)	2.030(6)		
O9(x3)	1.993(6)	O2(x2)	2.030(6)		
mean	1.992	*mean*	2.030		
V	4.06	*V*	4.29		
σ^2	0.01	σ^2	1.48		
λ	1.0000	λ	1.0004		

Note: the octahedral angle variance (σ^2) and the octahedral quadratic elongation (λ) were calculated according to Robinson et al. (1971).

TABLE 7 – Pure T-O and M-O reference bond lengths (Å) used to obtain calculated bond distances

	* Mn^{2+}	* Mg	* Zn	* Fe^{3+}	* Al	* Si	# Sb^{5+}
T-O	2.036	1.966	1.960	1.875	-	1.627	-
M-O	2.191	2.082	-	2.025	1.908	-	1.958

Notes: *data from the set of optimized distances proposed by Lavina et al. (2002);
the <M1-O> distance (this work) was used as pure Sb^{5+}-O.

TABLE 8 – Assumed cation populations in the different sites of the filipstadite structure

M1	1.00 Sb^{5+}
M2	0.20 Mg + 0.16 Mn^{2+} + 0.06 Fe^{3+} + 0.01 Al + 0.57 Sb^{5+}
M3	0.34 Mg + 0.29 Mn^{2+} + 0.11 Fe^{3+} + 0.01 Al + 0.25 Sb^{5+}
M4	0.63 Mg + 0.37 Mn^{2+}
M5	0.42 Mg + 0.34 Mn^{2+} + 0.14 Fe^{3+} + 0.01 Al + 0.09 Sb^{5+}
M6	0.35 Mg + 0.30 Mn^{2+} + 0.12 Fe^{3+} + 0.01 Al + 0.22 Sb^{5+}
T1	0.21 Mg + 0.79 Fe^{3+}
T2	0.96 Mn^{2+} + 0.04 Zn
T3	0.87 Fe^{3+} + 0.13 Si
T4	0.23 Mg + 0.77 Fe^{3+}
T5	0.05 Mg + 0.77 Mn^{2+} + 0.18 Fe^{3+}

TABLE 9 - Bond-valence (*v.u.*) arrangement for filipstadite.

	M1	M2	M3	M4	M5	M6	T1	T2	T3	T4	T5	Σ O
O1			$0.491^{x2\downarrow x2\rightarrow}$			$0.461^{x3\downarrow x1\rightarrow}$					$0.510^{x2\downarrow x1\rightarrow}$	1.95
O2		$0.630^{x1\downarrow x1\rightarrow}$			$0.412^{x2\downarrow x2\rightarrow}$						$0.510^{x2\downarrow x1\rightarrow}$	1.96
O3		$0.647^{x2\downarrow x1\rightarrow}$	$0.475^{x2\downarrow x1\rightarrow}$		$0.394^{x2\downarrow x1\rightarrow}$			$0.479^{x2\downarrow x1\rightarrow}$				2.00
O4		$0.626^{x1\downarrow x1\rightarrow}$		$0.389^{x2\downarrow x2\rightarrow}$			$0.522^{x3\downarrow x1\rightarrow}$					1.93
O5	$0.958^{x6\downarrow x1\rightarrow}$			$0.321^{x2\downarrow x2\rightarrow}$				$0.455^{x1\downarrow x1\rightarrow}$				2.06
O6						$0.454^{x3\downarrow x3\rightarrow}$				$0.519^{x1\downarrow x1\rightarrow}$		1.88
O7		$0.633^{x2\downarrow x2\rightarrow}$		$0.298^{x1\downarrow x1\rightarrow}$				$0.460^{x1\downarrow x1\rightarrow}$				2.02
O8			$0.464^{x1\downarrow x3\rightarrow}$				$0.506^{x1\downarrow x1\rightarrow}$					1.90
O9			$0.486^{x1\downarrow x1\rightarrow}$		$0.433^{x2\downarrow x2\rightarrow}$					$0.511^{x3\downarrow x1\rightarrow}$		1.86
O10				$0.420^{x1\downarrow x3\rightarrow}$					$0.708^{x4\downarrow x1\rightarrow}$			1.97
	5.75	3.82	2.88	2.14	2.48	2.75	2.07	1.87	2.83	2.05	2.04	

Note: calculated from the bond-valence curves of Brese and O'Keeffe (1991)